

New Selection Rules for Resonant Raman Scattering on Quantum Wires.

E. MARIANI (*)¹, M. SASSETTI¹, AND B. KRAMER²

¹ Dipartimento di Fisica, INFM, Università di Genova

Via Dodecaneso 33, I-16146 Genova, Italy

² I. Institut für Theoretische Physik, Universität Hamburg
Jungiusstraße 9, D-20355 Hamburg, Germany

(received dd July 1999; accepted dd Month 1999 in final form)

PACS. 71.45.-d – Collective effects.

PACS. 78.30.-j – Infrared and Raman spectra.

PACS. 73.20Dx – Electron stated in low-dimensional structures.

Abstract. – The bosonisation technique is used to calculate the resonant Raman spectrum of a quantum wire with two electronic sub-bands occupied. Close to resonance, the cross section at frequencies in the region of the inter sub-band transitions shows distinct peaks in *parallel polarisation* of the incident and scattered light that are signature of collective higher order *spin density excitations*. This is in striking contrast to the conventional selection rule for non-resonant Raman scattering according to which spin modes can appear only in perpendicular polarisation. We predict a new selection rule for the excitations observed near resonance, namely that, apart from charge density excitations, only spin modes with positive group velocities can appear as peaks in the spectra in parallel configuration close to resonance. The results are consistent with all of the presently available experimental data.

Raman spectroscopy is one of the most powerful experimental techniques for investigating the dispersion relation of elementary excitations in condensed matter [1, 2]. Recently, the spectra of the strongly correlated electrons in quantum wires [3, 4, 5] have been the subject of considerable experimental effort. It has been suggested that intraband charge and spin density excitations (CDE and SDE) which are signature of Luttinger liquid behaviour [6] can be identified in parallel and perpendicular polarisations of incoming and scattered light, respectively. In addition, the peaks in the polarised *resonant* Raman spectra, when the energy of the incident photon approaches the energy gap, that were associated so far with “single particle excitations” (“SPE”) have been identified as collective, higher order spin density excitations in the region of the *intraband* modes [7]. In order to treat the interband spectra, the bosonisation approach has been generalised to include interband coupling terms [8]. It has been shown that the essential experimental features observed *far from resonance* in the

(*) present address: I. Institut für Theoretische Physik, Universität Hamburg
Jungiusstraße 9, D-20355 Hamburg, Germany.

polarised and depolarised configurations of the light beams, in the frequency region of the lowest *interband* CDE and SDE, can be recovered.

In the present paper, we show that in the region of the interband transitions, higher-order SDE give rise to pronounced peaks in the resonant Raman spectra in *parallel polarisation*, in analogy with those found for the intraband modes (so-called “SPE”). We predict that these peaks are subject to a new selection rule: only interband SDE with a positive group velocity can appear in the resonant Raman spectra in the *parallel configuration* as sharp peaks. All of the presently available experimental data of quantum wires are completely consistent with our predictions. Nevertheless, more detailed experimental investigations, especially on quantum wires with two sub-bands, are necessary in order to confirm our results quantitatively. This would provide further strong evidence for the importance of the Coulomb interaction and the collective and bosonic nature of the electronic excitations in quantum wires which are signature of Luttinger liquid behavior [9].

We consider a quantum wire of length L (periodic boundary conditions) with two occupied conduction sub-bands with dispersion relations $E_i(k) = \varepsilon_i + \hbar^2 k^2 / 2m$ ($i = 1, 2$) where $\varepsilon_1 = 0$, $\varepsilon_2 = E_0$, E_0 the intersub-band separation, and m the effective mass of an electron in the conduction band. The position of the Fermi level E_F defines the Fermi velocities $v_{F1,2}$ corresponding to the two sub-bands. We assume a three dimensional (3D) Coulomb interaction. When projected with the confining wave functions onto the sub-bands, this gives the effective 1D interaction between the electrons [7]. The Hamiltonian of the free electrons in terms of Fermion operators $c_{is}^\dagger(k)$, $c_{is}(k)$ (spin s and wave number k) is

$$H_0 = \sum_{i=1}^2 \sum_{s,k} E_i(k) c_{is}^\dagger(k) c_{is}(k) \quad (1)$$

and the interaction energy

$$H_{\text{int}} = \sum_{ijlm} \sum_{ss'} \sum_{qkk'} V_{ijlm}(q) c_{is}^\dagger(k+q) c_{js'}^\dagger(k') c_{ls'}(k'+q) c_{ms}(k) \quad (2)$$

where $V_{ijlm}(q)$ are the matrix elements of the interaction potential.

In order to diagonalise this Hamiltonian, we use a generalisation of the Luttinger model which is commonly employed to describe the small-momentum collective excitations of 1D systems of interacting electrons [10]. The presence of two sub-bands allows pair excitations both within a given sub-band (*intraband* excitations) and between different sub-bands (*interband* excitations). As for the Luttinger model, we linearise the dispersion relations near the Fermi level. One obtains two spectral branches $\lambda = \pm$ for right/left-moving electrons. The Hamiltonian can then be diagonalised in terms of the density operators $\rho_{ij,s}^\lambda(q) = \sum_k c_{is}^{\lambda\dagger}(k+q) c_{js}^\lambda(k)$.

By using a mean field assumption the Hamiltonian can be decomposed into *independent* intraband and inter-band contributions [8] with independent charge and spin densities

$$\rho_{ij} = \rho_{ij,\uparrow} + \rho_{ij,\downarrow}, \quad \sigma_{ij} = \rho_{ij,\uparrow} - \rho_{ij,\downarrow} \quad (3)$$

respectively, similar to the one-band Luttinger model. The Coulomb repulsion affects the CDE while the SDE feel only the exchange interaction. The system can be diagonalised by using a generalised Bogolubov transformation [11]. For parameters characteristic for state-of-the-art semiconductor quantum wires [3, 12], the dispersion relations are shown in Fig. 1a.

The four energetically lowest branches of the spectrum correspond to the intraband charge and spin density modes, $\text{CDE}_0^{+,-}$ and $\text{SDE}_0^{+,-}$, respectively. The two lowest branches are the SDE. They are linear in the wave number with slopes approximately equal to the Fermi

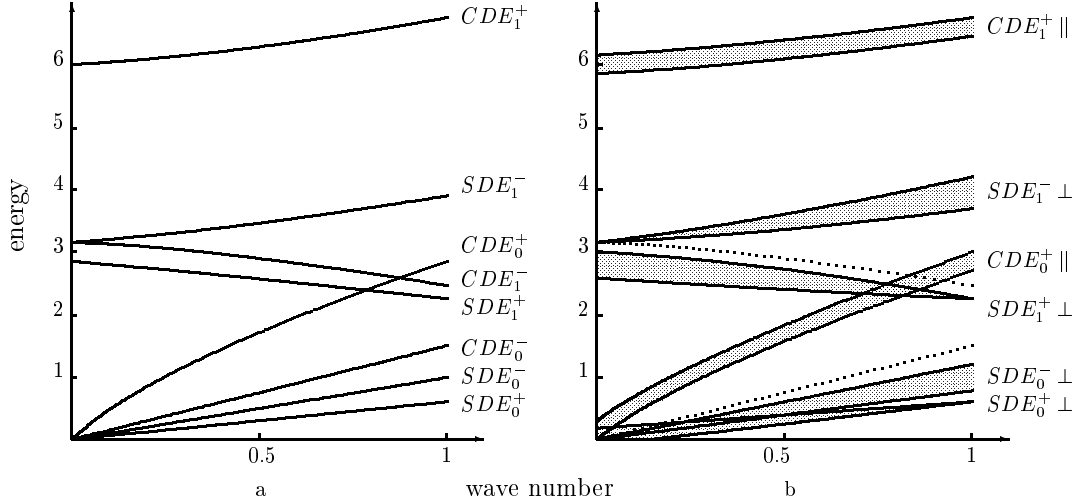


Fig. 1. – (a) Dispersion relations of intra- and inter-band CDE and SDE of the two-band Luttinger model. Energy in meV; wave number in 10^5 cm^{-1} . We chose $\hbar v_{F1} = 10^{-5} \text{ meV}\cdot\text{cm}$ and $v_{F2} = 0.6 v_{F1}$. (b) Frequency-wave number dependence of the peaks in the non-resonant Raman spectra for the modes shown in (a). In parallel polarisation of incoming and scattered light, only intra- and interband charge density modes, CDE_0^\pm and CDE_1^\pm (\pm symmetric and anti-symmetric excitations) can be observed. In perpendicular polarisation, SDE_0^\pm and SDE_1^\pm appear. Widths of the shaded areas: approximate intensity of the peaks in the Raman cross section. Dotted branches: intensity of Raman peaks unobservably small.

velocities $v_{F1,2}$ since the exchange interaction is very small. The next-higher two branches, starting again at $\omega = 0$ when $q = 0$, are the charge density modes. The uppermost intraband CDE, symmetric in the charge densities of the two sub-bands, reflects the Fourier-transform of the interaction, $\omega(q) \approx |q| (v_{F1} + v_{F2}) [1 + 2V_{1111}(q)/\pi\hbar(v_{F1} + v_{F2})]^{1/2}$ in the limit of long wave length [6, 7]. The slope of the energetically lower (anti-symmetric) CDE is proportional the geometrical average of the two Fermi velocities, $\omega(q) \propto (v_{F1}v_{F2})^{1/2} |q|$ [6, 7].

The four modes which start at $q = 0$ with finite frequencies are interband charge and spin excitations. The highest branch with the positive group velocity $d\omega(q)/dq$ corresponds to a symmetric interband charge density mode $\approx \rho_{12}^+ + \rho_{12}^-$. It is strongly shifted to higher energy by the Coulomb repulsion (depolarisation shift). The anti-symmetric branch, $\approx \rho_{12}^+ - \rho_{12}^-$, does not feel the Coulomb repulsion at small wave numbers and has a negative group velocity. It is degenerate with the anti-symmetric interband SDE, $\approx \sigma_{12}^+ - \sigma_{12}^-$ at $q = 0$, at an energy which is given by the interband spacing E_0 plus the exchange energy V_{ex} . In our example (Fig.1) $E_0 = 3 \text{ meV}$ and $V_{\text{ex}} \approx 0.2 \text{ meV}$. The two remaining branches of the spectrum correspond to the symmetric and anti-symmetric SDE ($\approx \sigma_{12}^+ \pm \sigma_{12}^-$), starting at $\hbar\omega \approx E_0 \mp V_{\text{ex}}$, respectively.

The differential cross section for the inelastic scattering of the light is given by Fermi's golden rule and can be written in terms of a response function $\chi(q, \omega)$ [2],

$$\frac{d^2\sigma}{d\Omega d\omega} = \left(\frac{e^2}{mc^2} \right)^2 \frac{\omega_O}{\omega_I} \frac{n(\omega) + 1}{\pi} \text{Im}\chi(q, \omega) \quad (4)$$

with $\omega = \omega_I - \omega_O$ the difference between the frequencies of the incident and scattered photons,

$q = k_I - k_O$ the transferred wave number, $n(\omega)$ the Bose distribution, and

$$\chi(q, t) = i \Theta(t) \langle [N^\dagger(q, t), N(q, 0)] \rangle \quad (5)$$

where $\langle \dots \rangle$ is the thermal average.

The operator

$$N(q, t) = \gamma_0 \sum_{ij,s} \sum_{\lambda,k} \frac{(e_I \cdot e_O + i |e_I \times e_O| s)}{D_i(k, q)} c_{is}^{\lambda\dagger}(k + q, t) c_{js}^{\lambda}(k, t) \quad (6)$$

is a generalised density describing an electronic excitation of momentum q from band j to band i in the branch λ . The vectors $e_{I,O}$ indicate the polarisation of the incoming/outgoing photon, the constant γ_0 contains the matrix elements for the transitions between the valence and the conduction band, and the energy denominator

$$D_i(k, q) = E_i(k + q) - E_v(k + q - k_I) - \omega_I \quad (7)$$

where E_v is the energy of the valence band that will be assumed as dispersion-less. We calculate the above generalised density by using the bosonization method [7] and expanding D^{-1} in powers of $E_F/(E_g + \varepsilon_i - \hbar\omega_I + \lambda\hbar v_{F12}q/2)$ ($E_g = E_g^0 + \hbar^2 k_{F12}^2/2m$). Here, we have defined an average Fermi wave number, $k_{F12} = (k_{F1} + k_{F2})/2$, with the corresponding average Fermi velocity $v_{F12} = \hbar k_{F12}/m$.

If the energy of the incident photon is sufficiently high, we are far from resonance and can consider only the lowest order term in the expansion of D^{-1} . This gives

$$N(q, t) = \sum_{ij,\lambda} \frac{\gamma_0}{E_g + \varepsilon_i - \hbar\omega_I + \lambda\hbar v_{F12}q/2} [e_I \cdot e_O \rho_{ij}^\lambda(q, t) + i |e_I \times e_O| \sigma_{ij}^\lambda(q, t)]. \quad (8)$$

This implies the “classical selection rule” for Raman scattering: only CDE can appear in the polarised configuration and SDE can only be present in the depolarised one. The behaviour of the peaks in the frequency-wave number plane to be expected for the non-resonant Raman spectra, $|E_g - \hbar\omega_I| \gg \varepsilon_i + \lambda\hbar v_{F12}q/2$ has been discussed earlier [8]. An overview based on the quantitative results from our model calculation is given in Fig. 1b. Remarkably, the anti-symmetric charge excitations denoted as CDE_0^- and CDE_1^- turn out to have a very small intensity such that they cannot be observed far from resonance [7]. Similarly, the symmetric spin excitations SDE_0^+ and SDE_1^+ can at best be observed at small wave numbers while SDE_0^- and SDE_1^- will be present at larger wave numbers. As the intraband SDE are close in frequency, the experiment will show one peak which increases in frequency almost linearly with q .

Although this is only the first term in the expansion, we nevertheless have to take into account its contribution towards the spectra when we consider photon energies closer to resonance. Indeed, when $|E_g + \varepsilon_i - \hbar\omega_I| \approx \hbar v_{F12}q/2$ the term can contribute considerably. The behaviour in frequency-wave number space of the Raman peaks corresponding to the inter-band transitions according to this zero-order term is shown in Fig. 2a [8]. In parallel polarisation, only CDE are observable: CDE_1^- is expected to dominate at small q , and CDE_1^+ becomes strong for larger q . In perpendicular configuration, only SDE_1^- is expected.

Using the bosonic representation of the fermionic operators in Eq. (6), the first-order contribution to $N(q, t)$ is

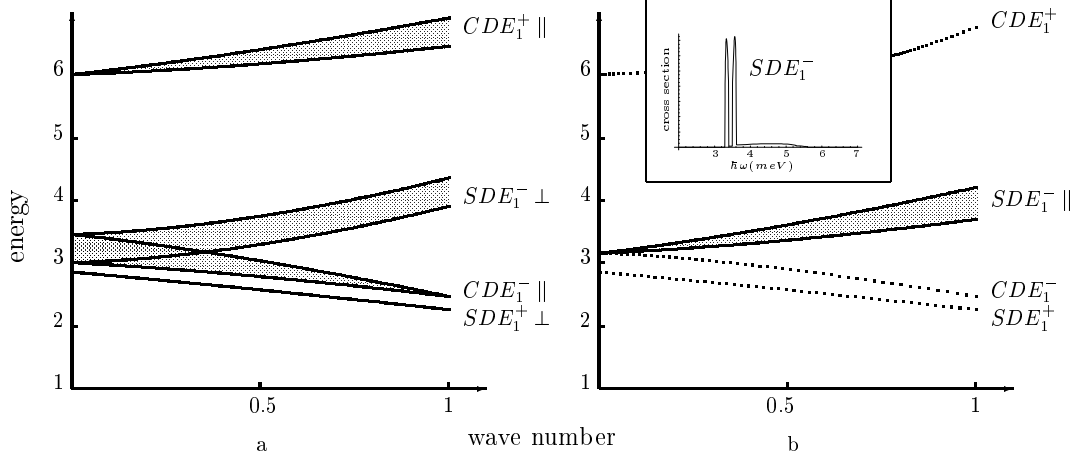


Fig. 2. – (a) Behaviour in frequency-wave number space of the inter-band resonant Raman peaks according to the zero-order term in Eq. (8); energy in meV; wave number in 10^5 cm^{-1} . (b) Inter-band resonant Raman peaks for polarised configuration from the first-order term (Eq. (9)); widths of shaded areas: intensities of the peaks in the Raman cross section. Dotted branches: intensity of Raman peaks unobservably small. Inset: Raman cross section (arbitrary units) for the inter-band SDE for $T = 0$, with $\hbar v_{F1} = 10^{-5} \text{ meV}\cdot\text{cm}$, $v_{F2} = 0.6 v_{F1}$, evaluated at $q = 0.8 10^5 \text{ cm}^{-1}$. Notice the pronounced double peak structure which is due to the inter-band mode with positive group velocity (SDE_1^-). The flat background-structure between $\hbar\omega \approx 3.5 \text{ meV}$ and $\hbar\omega \approx 5.5 \text{ meV}$ is related to SDE_1^+ .

$$\begin{aligned} \Delta N(q, t) &= -\frac{\pi}{2L} \frac{\gamma_0 \hbar^2}{m} \sum_{ij,\lambda} \frac{k_{F12} + \lambda q/2}{[E_g + \varepsilon_i - \hbar\omega_I + \lambda \hbar v_{F12} q/2]^2} \times \\ &\quad \times \sum_{k,l} \left\{ (\mathbf{e}_I \cdot \mathbf{e}_O) [\rho_{ll}^\lambda(q-k, t) \rho_{ij}^\lambda(k, t) + \sigma_{ll}^\lambda(q-k, t) \sigma_{ij}^\lambda(k, t)] + \right. \\ &\quad \left. + i |\mathbf{e}_I \times \mathbf{e}_O| [\rho_{ll}^\lambda(q-k, t) \sigma_{ij}^\lambda(k, t) + \sigma_{ll}^\lambda(q-k, t) \rho_{ij}^\lambda(k, t)] \right\}. \end{aligned} \quad (9)$$

The intraband case ($i = j$) has already been studied in detail and can be treated within the one band Luttinger model [7]. It has been found that the spin density operators present in the polarised term ($\propto \mathbf{e}_I \cdot \mathbf{e}_O$) give rise to Raman peaks that violate the classical selection rule, since they appear in parallel polarisation. In previous works, these have been associated with “single particle excitations”.

The present two-band model specifically allows for investigating the behaviours of the inter-band modes closer to resonance. The polarised terms in Eq. (9) ($\propto \mathbf{e}_I \cdot \mathbf{e}_O$) are bi-linear in the spin density operators and yield the dominant contribution to the Raman cross section. An important feature is that they couple directly inter- and intraband modes.

By writing them in terms of the eigen-modes of the Hamiltonian, for which the time evolutions are known, and by evaluating the response function Eq. (5) we obtained a closed expression for $d^2\sigma/d\Omega d\omega$. Figure 2b shows the behaviour in frequency-wave number space of the possible interband Raman peaks according to the first-order term, Eq. (9). Only the anti-symmetric spin mode SDE_1^- contributes in parallel polarisation! Due to the mixing of this inter-band mode which has a positive group velocity with the two intraband SDE related to

the two Fermi velocities a double peak appears in the spectrum at zero temperature (Fig. 2b inset). The width of the peaks is roughly proportional to the difference between the group velocities of the coupled modes and they are centred on two lines with slopes equal to the two Fermi velocities v_{F1} and v_{F2} , starting around $E_0 + V_{\text{ex}}$. For non-zero temperatures, the two peaks are smeared and appear as only one structure. The presence of disorder will also broaden the peaks. The resulting SDE-peak in the parallel configuration appears roughly at the frequency of the SDE_1^- , and its intensity increases with increasing wave number as indicated by the increasing width of the shaded area in Fig. 2b.

On the other hand, by coupling the inter-band spin mode with negative group velocity to the two intraband spin density excitations we obtain a very flat and broad structure (Fig. 2b inset) that will not be observable experimentally.

In the terms in Eq. (9) which correspond to perpendicular polarisation ($\propto \mathbf{e}_I \times \mathbf{e}_O$) charge and spin density operators are mixed. These contribute towards the Raman cross section only with broad structures within frequency windows that are given by the differences of the group velocities of the modes that are mixed. They are not expected to be experimentally detectable.

In summary, we have evaluated the Raman cross section of a semiconductor quantum wire with two conduction sub-bands occupied by using the bosonisation method for two coupled Luttinger liquids. We have found strong violations of the “classical selection rules” for Raman scattering. Due to higher order terms which become important when the energy of the incident photons approaches the energy gap between conduction and valence band of the semiconductor, SDE modes appear in perpendicular as well as in parallel polarisation of incident and scattered photons. For these, a novel selection rule has been established: only SDE which can combine with intraband modes with similar group velocities can occur in parallel polarisation as distinct peaks. On the other hand, in perpendicular configuration, no higher-order CDE modes become observable.

Our model allows to understand the physical reason for this selection rule: coupling between an inter-band SDE with positive group velocity and intraband modes which have group velocities (\approx Fermi velocity) leads to a long-range correlation in time between the corresponding collective excitations. As a consequence, $\chi(q, \omega)$, the Fourier transformed correlation function, will show a pronounced structure in (q, ω) -space. On the other hand, due to opposite signs of the group velocities of the inter-band mode SDE_1^+ and of the two intraband excitations, the correlation in time is short-range. Its Fourier transform will be long-range in frequency. A similar qualitative argument explains also the *absence* of pronounced, sharp peaks in perpendicular polarisation due to the combined spin-charge excitations which have necessarily very different group velocities. As the origin of structure in perpendicular polarisation is related to spin-orbit coupling, no higher-order CDE alone can occur. Only higher-order CDE accompanied by at least one SDE are present. This physical argument suggests that the new selection rule is very probably also valid for more than two sub-bands.

Our findings are consistent with existing Raman data of two-band quantum wires [3], where the structures violating the selection rules have been denoted as “single particle excitations”. However, more precise measurements are needed in order to verify our quantitative predictions concerning, for instance, the dependence of the peak intensities on wave number and frequency (Fig. 2).

In conclusion, previous and present experimental and theoretical findings indicate that the observed features in the Raman spectra of quantum wires seem to be completely understandable in terms of the collective intra- and inter-band spin and charge excitations characteristic of coupled Luttinger liquids. This represent in our opinion strong evidence that the Luttinger model in connection with bosonisation correctly describes the collective modes in quantum wires for $q \neq 0$. Whether or not this is also valid for $q \rightarrow 0$ (near $T = 0$) is an open question

and presently intensively discussed [13, 14, 15].

Acknowledgements: We thank Franco Napoli for useful discussions. The work has been supported by the Italian MURST Cofin 98, the Deutsche Forschungsgemeinschaft via SFB 508 and Graduiertenkolleg “Nanostrukturierte Festkörper” of the Universität Hamburg, and by the EU via the TMR programme.

REFERENCES

- [1] PINCZUK A. and ABSTREITER G., in: *Light Scattering in Solids V, Topics in Applied Physics*, Vol. **66**, edited by CARDONA M. and GÜNTHERODT G., Springer Verlag, Heidelberg 1988 p. 153.
- [2] KLEIN M. V., in: *Light Scattering in Solids, Topics in Applied Physics*, Vol. **8**, edited by CARDONA M., Springer Verlag, Heidelberg 1975 p. 147.
- [3] GOÑI A. R. ET AL., *Phys. Rev. Lett.*, **67** (1991) 3298; and in: *Phonons in Semiconductor Nanostructures*, edited by LEBURTON J.P., PASCUAL J. and SOTOMAYOR-TORRES C., NATO ASI Ser. E Vol. **236** Plenum Press 1992 p. 287.
- [4] SCHMELLER A. ET AL., *Phys. Rev. B*, **49** (1994) 14778.
- [5] SCHÜLLER C. ET AL., *Phys. Rev. B*, **54** (1996) R17304.
- [6] SCHULZ H. J., *Phys. Rev. Lett.*, **71** (1993) 1864.
- [7] SASSETTI M. and KRAMER B., *Phys. Rev. Lett.*, **80** (1998) 1485; *Eur. Phys. J. B*, **4** (1998) 357.
- [8] SASSETTI M., NAPOLI F. and KRAMER B., *Phys. Rev. B*, **59** (1999) 7297.
- [9] SASSETTI M. and KRAMER B., *Ann. Phys. (Leipzig)*, **7** (1998) 508.
- [10] LUTTINGER J. M., *J. Math. Phys.*, **4** (1963) 1154; HALDANE F. D. M., *J. Phys C*, **14** (1981) 2585; VOIT J., *Rep. Progr. Phys.*, **57** (1995) 977.
- [11] PENC K. and SOLYOM J., *Phys. Rev. B*, **47** (1993) 6273.
- [12] SASSETTI M. ET AL., in: *Procs. ICPS24, Jerusalem 1998*, World Scientific Publ., Singapore 1999 p. CD VII B-19.
- [13] FINKEL'STEIN A. M. and LARKIN A. I., *Phys. Rev. B*, **47** (1993) 10461.
- [14] FABRIZIO M., *Phys. Rev. B*, **48** (1993) 15838.
- [15] SCHULZ H. J., *Phys. Rev. B*, **53** (1996) R2959.